Textile Research Journal

Original article

Textile Research Journal
0() 1–11

DOI: 10.1177/0040517520966733
journals.sagepub.com/home/trj
SAGE

Semi-supervised fabric defect detection based on image reconstruction and density estimation

Qihong Zhou[1], Jun Mei[1], Qian Zhang[2], Shaozong Wang[2] and Ge Chen[1]

Abstract

Defective products are a major contributor toward a decline in profits in textile industries. Hence, there are compelling needs for an automated inspection system to identify and locate defects on the fabric surface. Although much effort has been made by researchers worldwide, there are still challenges with computation and accuracy in the location of defects. In this paper, we propose a hybrid semi-supervised method for fabric defect detection based on variational autoencoder (VAE) and Gaussian mixture model (GMM). The VAE model is trained for feature extraction and image reconstruction while the GMM is used to perform density estimation. By synthesizing the detection results from both image content and latent space, the method can construct defect region boundaries more accurately, which are useful in fabric quality evaluation. The proposed method is validated on AITEX and DAGM 2007 public database. Results demonstrate that the method is qualified for automated detection and outperforms other selected methods in terms of overall performance.

Keyword

fabric defect detection, anomaly detection, variational autoencoder, image reconstruction, Gaussian mixture model, density estimation

Introduction

In addition to fulfilling people's clothing needs, textiles are widely sought after in other industries, such as aerospace,[1] water treatment,[2] geotechnical,[3] and biomedical science.[4] Although the textile industry has employed various technologies over the years, defects can occur in textile products. Common defects include broken yarn, weft cracks, and creases. Evidently, these issues can adversely affect the competitiveness of textile businesses.

Therefore, it is necessary to perform defect detection in the fabric production process. Companies currently prefer automated visual inspection systems to traditional human vision, which is both inefficient and expensive. A system equipped with lighting, industrial cameras, and detection algorithms can give real-time warning signals of defective products on the production line. Moreover, these systems can provide extensive quantitative data on fabric defects, which is highly effective in the optimization of subsequent production parameters. Automated fabric inspection has been one of the most popular research areas over the past 30 years, and many efforts[5–7] have been made by researchers from different institutions to develop effective approaches. These approaches can be classified into four categories:[8] statistical, spectral, model-based, and learning-based. Compared with the tedious work in feature engineering, machine learning can acquire better feature representation without much effort, and has begun to play a greater role in fabric inspection.

With the rapid development of deep learning (DL), there are many emerging methods for fabric inspection.

[1]College of Mechanical Engineering, Donghua University, China
[2]Beijing National Innovation Institute of Lightweight Ltd., China

Corresponding author:
Qihong Zhou, Donghua University, 2999 North Renmin Road, Songjiang, Shanghai 201620, China.
Email: zhouqihong@dhu.edu.cn

In brief, these methods can be grouped into three computer vision tasks: image classification,[9] object detection,[10] and semantic segmentation.[11] The classification task gives an overall content description of test images and then assigns certain labels to them. The detection task aims to distinguish specific objects and creates bounding boxes around them. For this purpose, location information for objects is also essential, which can be obtained by adopting a sliding window or selective search algorithm. Segmentation can be regarded as pixel-level classification. Compared with other two tasks, semantic segmentation is capable of precise quantitative evaluation. There are many unique models in this research area, such as FCN-16s, U-Net, and Mask R-CNN. Certainly, a pixel-wise labeled dataset is essential for end-to-end training.

The biggest challenge for application of DL is the dataset. Without training data, even elegant model design is essentially useless. The lack of a complete dataset mostly depends on the following factors: (1) expensive human labeling; and (2) extremely imbalanced datasets. In general, factories have ample facility for defect-free production while the occurrence of defects in fabrics is a small probability event. Conversely, it is feasible for fabric-related datasets to be totally composed of positive samples. Hence, transforming the fabric inspection into anomaly detection in images can provide a solution to the problem.[12] This type of detection mode could be loosely separated between data mining and reconstruction-based techniques.

Traditional anomaly-detection algorithms can be simply applied to images via some technological means. Test images need to be processed into structured data firstly as a premise, which is convenient for the execution of algorithms. For example, convolutional neural network is most popularly used for automated feature extraction nowadays.[13,14] Consequently, defects will be detected by thresholding after calculating the anomaly probability of test samples. Anomaly-detection algorithms are usually grouped into four categories: statistical based, density based, distance based, and clustering based. Statistical-based methods identify outliers with tests for inconsistency by assuming that the dataset is subject to a certain model. Density-based methods define objects in low-density areas as outliers. Distance-based methods affirm that the distance between an outlier and other normal points is greater than the set threshold. Clustering-based methods define points which fall into smaller clusters as outliers. By way of illustration, Napoletano et al.[15] performed feature extraction by utilizing a pre-trained ResNet-18 model. Anomalies in fabric images were then detected by means of dictionary and statistics. The method has done a good job on a public SEM fabric dataset, yielding and area-under-the-curve (AUC) value of 0.926.

The implementation of reconstruction-based anomaly detection depends on the image generative model, namely autoencoder (AE) or generative adversarial network (GAN).[16] In general, GAN provides clearer reconstruction with a harder training process. An image-generation model is eligible to correctly reconstruct anomalous images by learning from plenty of normal samples. In other words, the defect regions in images are repaired as accurately as possible and can be easily detected by comparing original and repaired images. In recent years, researchers have made many attempts in that direction. Haselmann et al.[17] designed an AE and trained its capability of image completion, yielding an average AUC of 0.985 on the decorated parts dataset. Zhao et al.[18] proposed a defect-detection framework based on training of only positive samples with AE, and obtained a mean accuracy of 94.43% on the DAGM 2007 fabric dataset. Besides AEs, there have been many improvements to the vanilla GAN for the purpose of anomaly detection. Schlegl et al.[19] and Zenati et al.[20] proposed AnoGAN and Efficient-GAN successively around 2017. Afterwards, Akcay et al.[21] proposed GANomaly by creatively employing encoder-decoder-encoder sub-networks in the generation network, which shows contemporary state-of-art performance on the UBA and FFOB datasets.

In this paper, we propose a novel semi-supervised method for fabric defect detection based on variational autoencoder (VAE)[22] and Gaussian mixture model (GMM).[23,24] The design of method is mainly inspired by Hu et al.[25] and GANomaly,[21] which detect defects on the basis of both image content and latent space. The hybrid strategy for fabric inspection has been proved effective and superior experimentally. First, we constructed a VAE network and trained it only with positive samples. The VAE was used to perform reconstruction and feature-extraction functions of a given image. In this step, potential defect regions could be designated using a structural similarity index (SSIM)[26,27] to quantify difference between the original and the reconstructed images. Then, we incorporated a GMM to feature vectors from the encoder in VAE. The anomaly detection was performed with density estimation[28] for this step, that is, defective products tend to obtain lower probability density compared with positive samples. Eventually, the two methods for defect detection are fused to produce a better result.

Problem formulation

To fulfill the needs of both qualitative and quantitative analysis in textile enterprise, the defect regions should be recognized and located. In other words, fabric defect detection could also be described as an implementation of segmentation function in fabric images.

We define the grayscale image of fabric I (as shown in Figure 1(a)) as a matrix Φ of size $w \times h$, thus, the value $\alpha(0 \le \alpha \le 255)$ of $\Phi(x,y)(0 \le x < w, 0 \le y < h)$ can represent the pixel value of each corresponding point in the image. Therefore, the problem of fabric defect detection is transformed into looking for such a matrix Ω whose size is equal to Φ in the meantime of $\forall x,y$,

$$\Omega(x,y) = \begin{cases} 0, & if\ \Phi(x,y) \notin anomalous\ pixels \\ 1, & if\ \Phi(x,y) \in anomalous\ pixels \end{cases} \quad (1)$$

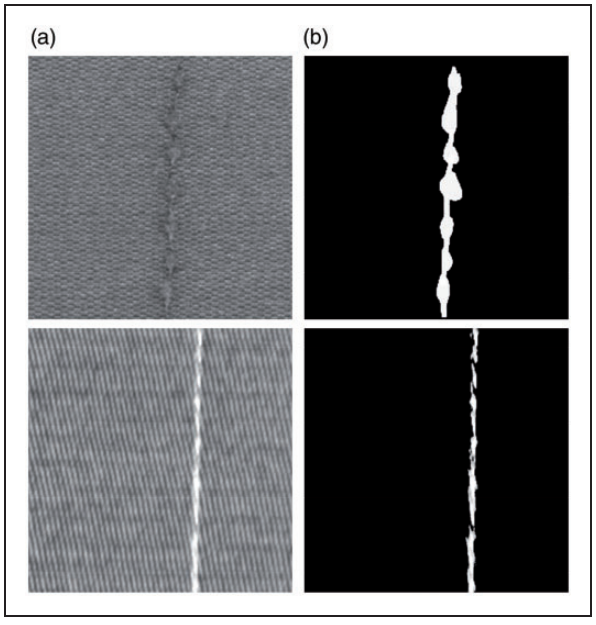

Figure 1. (a) fabric samples with defects *I*; (b) the corresponding ground-truth images Ω where white pixels represent defect regions.

Methodology

The proposed method was performed with a patch-wise manner, i.e. the test image was cut into patches I of same size prior to the actual process. We integrated image reconstruction with traditional algorithms aiming to acquire a better defect segmentation result. The two different methods produced difference map f_d and score map f_s, respectively, which can then be combined and processed to create a final segmentation map S. Furthermore, SSIM, weighted-HO operator, and morphological image processing were also applied to improve the performance of defect detection. Figure 2 shows the schematic diagram and the detailed practical aspects are discussed in three sections below.

Reconstruction and feature extraction

It is necessary to convert image data to tractable structured data when supervised learning techniques cannot be used for the lack of a labeled set. Although structured data can be obtained by directly flattening the image array of size $w \times h$ to a one-dimensional array, information regarding pixel positions will be lost during the conversion process. More seriously, high-dimensional feature vectors obtained in this way may lead to severe problems such as over-fitting.

Accordingly, we decided to perform this conversion using feature extraction,[29] anticipating that superior feature vectors can still maintain distinguishability. Feature-extraction algorithms for images can be classified into two generic groups: (1) traditional feature engineering, and (2) neural network. The first method usually extracts features from images through histogram of oriented gradients or scale-invariant feature transform. As texture, color, and shape of the images are involved, the optimal combination needs to be determined by experiments or from experience. Fortunately, owing to the emergence of deep

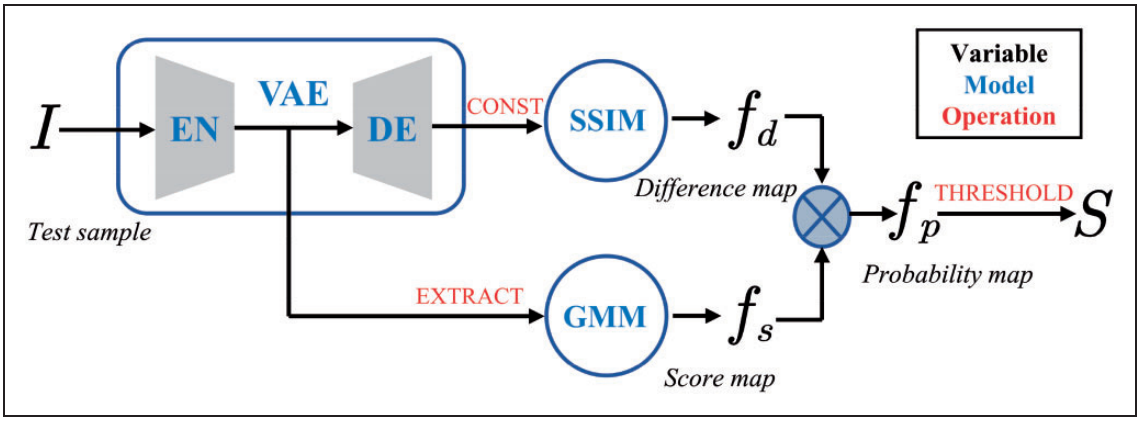

Figure 2. The framework of proposed detection method.

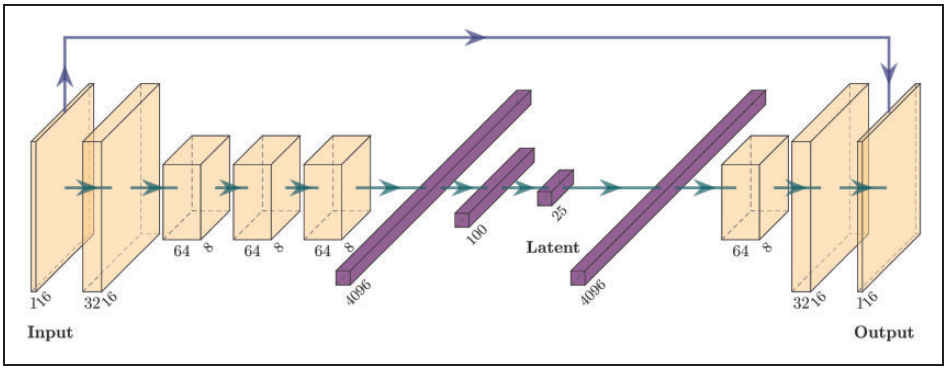

Figure 3. Schematic representation of the VAE model used. All test images are scaled to fit the input layer ($16 \times 16 \times 1$) before being fed into the model. The model is composed of 11 layers, where the dense layer (25) is utilized for feature extraction.

convolutional neural networks, feature extraction is no longer a tedious job. For example, it is also feasible to use the last few layers prior to the output of the pre-trained network as image features. The method is not only easy to operate but can also produce features which are expressive and discriminative.

VAE was finally chosen for implementing feature extraction as well as image reconstruction. An AE is a type of neural network applying the backpropagation algorithm to set the target values to be equal to the inputs. The encoder inside converts the input image into a latent space representation, while the decoder restores the representation to its original dimension. Obviously, the encodings can be regarded as another efficient expression of the original inputs. As early as 1986, Rumelhart et al.[30] adopted a similar approach for the analysis of high-dimensional data. VAE is a specific variation of the vanilla AEs. It integrates stacked convolutional layers instead of fully connected layers, which can retain vital pixel position information in addition to reducing excessive parameters. On the other hand, Gaussian noise and KL divergence loss are introduced into the VAE training process to attain a confrontation training, which is similar to GAN. The measure could thus achieve a robust decoding effect. Moreover, VAE can also provide decoupled feature vectors which are useful in subsequent process.

Figure 3 shows the typical network architecture (see Table 1 for further details) of the proposed approach. For the semi-supervised learning, there will be only defect-free fabric datasets engaged in the training process. In addition, the optimal latent space dimensions will be determined comprehensively by the quality of image reconstruction and the performance of defect detection. In the testing phase, we will obtain two different types of outputs after image of defective fabric (negative sample) is fed into the VAE. (1) Reconstructed image in image space: As VAE only learns how to reconstruct non-defective fabric images, defect regions in the defective images will be repaired as normal regions as possible. Hence, potential defect regions will be easily detected by comparing the original with the reconstructed image. (2) Feature vectors in latent space: It is a fact that anomalous images often manifest as abnormalities in the latent space, which may be the outliers of the whole feature vectors. Generally, the more anomalous a sample is, the greater deviation it shows.

Table 1. Architecture of proposed VAE model

Layer Name	Output Size	Number of parameters
Conv2D_1	$16 \times 16 \times 32$	320
Conv2D_2	$8 \times 8 \times 64$	18496
Conv2D_3	$8 \times 8 \times 64$	36928
Conv2D_4	$8 \times 8 \times 64$	36928
Flatten	4096	0
Dense_1	100	409700
Lambda	25	2525×2
Dense_2	4096	106496
Reshape	$8 \times 8 \times 64$	0
ConvTranspose2D	$16 \times 16 \times 32$	18464
Conv2D_5	$16 \times 16 \times 6$	289

Normal patches model

The VAE model built above provides the functionalities for image reconstruction and feature extraction. Though the reconstruction-based method is capable of indicating the defect regions, it is not sufficient as the method may be susceptible to random external factors. Hence, additional effort is essential to improve the robustness of the detection result. This can be done by adopting traditional anomaly-detection algorithms, an approach interpreted in detail hereinafter.

As positive samples and feature extractor are available, it is simple to transform fabric inspection into anomaly detection in images. As a typical problem in machine learning, there are various algorithms for anomaly detection, such as k-nearest neighbors (KNN), local outlier factor, and support vector machine. These algorithms mostly adopt unsupervised learning techniques owing to the peculiarity of anomaly detection in real life. Nevertheless, in view of the number of known positive samples, the anomaly detection is finally performed by means of fitting the data to a GMM.

GMM is often used in solutions that model the data with multiple distributions. As a type of clustering algorithm, it is widely applied to anomaly detection. Its form is expressed into the linear combination of multiple Gaussian distributions and corresponding probability density function is formulated as

$$p(x) = \sum_{i=1}^{K} \Phi_i \frac{1}{\sqrt{2\sigma_i^2 \pi}} e^{-\frac{(x-\mu_i)^2}{2\sigma_i^2}} \left(\Phi_i > 0, \sum_{i=1}^{K} \Phi_i = 1 \right) \quad (2)$$

where Φ_i serves as the weight factor of each independent Gaussian distribution. Actually, GMM is in essence an algorithm for density estimation (i.e. a generative probabilistic model describing the distribution of the data). If we just fit the GMM to the positive samples, GMM will also only learn probability distribution of normal data. On the contrary, negative samples will naturally fall into low-density regions and their degree of anomaly can be measured on the deviation from normal density.

Before fitting data with GMM, it is necessary to select the number of components for better clustering performance. The optimal number has a good balance between the stability and quality of the fitting procedure. To measure the quality of models, Akaike and Bayesian information criterion (AIC and BIC)[31,32] are often used. They are defined as follows:

$$\begin{cases} AIC = 2k - 2\ln(L) \\ BIC = k\ln(n) - 2\ln(L) \end{cases} \quad (3)$$

where k and n denote the number of components and samples, respectively, and L is the likelihood function. BIC is preferred as it models data with fewer parameters usually for tougher penalty terms. The optimal number of components is determined when BIC takes the minimum value. Once GMM is built and trained, the probability density of training and test samples can be calculated for anomaly estimation. For fear of overflow and right-skewed distribution, weighted log-probabilities will be adopted alternatively.

Generally, the smaller the density of a sample, the higher the probability of anomaly. However, there will be negative values as a result of logarithmic function. As the expression form is not relatively intuitionistic, the calculated density will be translated and scaled as the following formula:

$$s = 255 \cdot \frac{p_{\max} - p}{p_{\max} - p_{\min}} \quad (4)$$

where s and p denote the final anomaly score and the middle log probability. In this way, the value s can be directly utilized for measuring the degree of anomaly.

Segmentation of defect regions

This section introduces how defect regions are segmented from the original fabric images. The difference map (VAE-based) and score map (GMM-based) are constructed successively and combined into the final probability map, as detailed below.

The pre-trained VAE provides the functionality for image reconstruction. Figure 4(a) and 4(b) show the image of fabric with defects and the reconstructed image, respectively. The defect regions in Figure 4(b) have been repaired to the extent feasible, which can be perceived in an enlarged view. Figure 4(c), obtained through the difference between 4(a) and 4(b), indicates this. As it is difficult to perform perfect reconstruction in detail with VAE, troubling impulse noise spreads all over the residual map. Consequently, we applied the SSIM index algorithm for identifying differences between Figure 4(a) and 4(b). SSIM is a perceptual metric that measures the difference between two similar images from the perspective of brightness, contrast, and

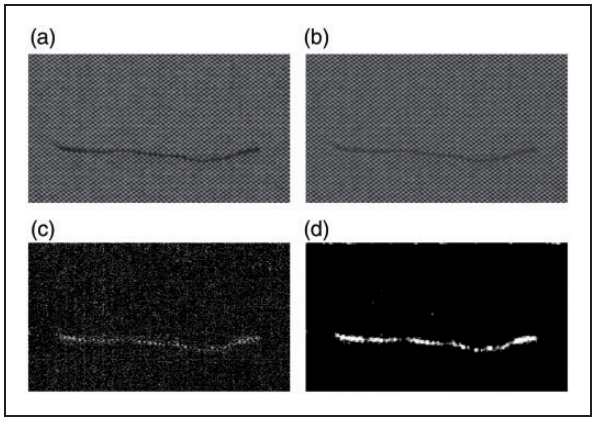

Figure 4. Comparison of the difference map from two methods: (a) the defective fabric sample; (b) the reconstruction image corresponding to (a); (c) the difference map from simple difference operation; (d) the difference map from SSIM method.

structure. The SSIM index of the original and reconstructed image was first calculated to generate the full SSIM image, where pixel values reflect the degree of difference. Then a clearer and more accurate difference map f_d was obtained ultimately by adopting Otsu thresholding, as shown in Figure 4(d). The difference map is a binary image where white and black pixels represent normal and defect regions, respectively.

With the aid of the GMM built above, the degree of anomaly on image patches can be evaluated. However, a pixel-level anomaly score map is really required for segmentation of defect regions. Under the premise of not rapidly increasing computational complexity, we improved the existing solutions which directly assign score of the patch to subordinate pixels. We proposed and applied the weighted-HO operator to the process of assignment, which is motivated by the algorithm for key-point localization.[33] The operator can be expressed for the following matrix: only variables within the central square region are set to one, while the value of other variables is inversely proportional to the distance from the center. Consequently, the final score matrix of patch can be readily obtained by calculating the dot product of the operator and the original one. Figure 5 shows a typical weighted-HO operator with a patch size of 8 pixels which is also applied to other situations through scaling. As the stride may be unequal to the size, each pixel of the image patch usually obtains anomaly score of more than one. In this case, we perform the average operation first and then draw the score map f_s.

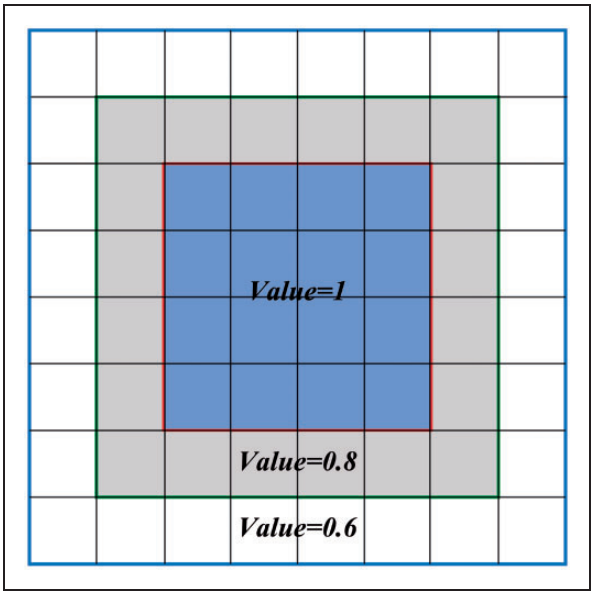

Figure 5. Schematic of a typical weighted-HO operator. Weight factor takes on the values 1.0, 0.8, 0.6 from inside to outside, respectively.

After completing the difference map and score map, the anomaly probability map f_p can be given by

$$f_p = \frac{\alpha \cdot f_d + \beta \cdot f_s}{\max(\alpha \cdot f_d + \beta \cdot f_s)} (\alpha, \beta > 0, \alpha + \beta = 1) \quad (5)$$

where α & β here are used for adjusting the weights of f_d & f_s. In the validation phase, the probability map f_p is compared with the corresponding ground-truth image to generate a threshold th. The value can be utilized in real-world applications as the following formula:

$$S = \begin{cases} 0, & f_p < th \\ 1, & f_p \geq th \end{cases} \quad (6)$$

where S denotes the segmentation map. More precisely, additional morphological operations are carried out to smooth the border of defect regions. As a result, the final segmentation map S is the matrix Ω sought in the "Problem formulation" section.

Experiments

The proposed method was evaluated on two public fabric datasets with multiple performance metrics. The experiments mainly explored the effects of patch size p and latent space dimension l on the computational complexity and detection accuracy. There are four alternative solutions adopted to show the superiority of proposed method. The method was implemented with TensorFlow 1.15,[34] which is an open source platform for DL. All experiments were conducted on a workstation mounting an Intel Xeon W-2155 @ 3.30GHz, 32GB RAM, and a NVIDIA Quadro P2000.

Dataset description

The images used in the experiments were mainly selected from the AITEX[35] fabric image database and the dataset of DAGM 2007.[36] The AITEX textile database is composed of seven different fabrics with 12 types of defects, and the original images have a size of 4096×256 pixels. In the database, each fabric image with defects corresponds to a pixel-level ground-truth image, which can be used for evaluation in this work. In fact, the database does not contain sufficient training images for perfect image restoration. This is one of the reasons for the adoption of a hybrid method in this paper. As a patch-wise anomaly detection method, all the original images were initially cut into image patches of the same size. Subsequently, we generated training, validation, and test sets from these patches. The training set includes only positive samples.

Performance metrics

The proposed method was evaluated by comparing segmentation map S with the ground truth Ω corresponding to the original image. To obtain the optimal segmentation map, a reasonable threshold is needed. It is insufficient to assess the performance using a single accuracy score for imbalanced datasets in anomaly detection. Therefore, several composite indices were used instead,[37] such as precision, AUC, and F-Score. Table 2 below introduces basal performance metrics which are frequently used for evaluating classifier.

Precision and sensitivity are widely used for performance evaluation when the data are extremely imbalanced, and are defined as follows:

$$\begin{cases} Precision = TP/(TP + FP) \\ Sensitivity = TP/(TP + FN) \end{cases} \tag{7}$$

Although higher precision and sensitivity usually mean better performance, there are contradictions and restrictions mutually between the two. As a consequence, F-Score is introduced for a comprehensive balance by considering both the precision and sensitivity. The measure is defined as the following formula:

$$F\_Score = (1 + \beta^2)\frac{Precision \cdot Sensitivity}{\beta^2 \cdot Precision + Sensitivity} \tag{8}$$

where $\beta(\beta > 0)$ is utilized to determine the weight of precision and sensitivity. In the context of anomaly detection, sensitivity is generally considered to be more important. Consequently, F_2 score is usually assigned with $\beta = 2$ and thus the F_2 score ranges from 0 to 1. The classifier offers the best performance when F_2 score reaches the highest value.

The receiver operating characteristic (ROC) curve is often used for the performance evaluation of a classification model as well. The graphical plot is illustrated by false positive rate (FPR) as X-axis and true positive rate (TPR) as Y-axis based on a series of thresholds. FPR and TPR are defined as the following formula:

$$\begin{cases} FPR = FP/(FP + TN) \\ TPR = TP/(TP + FN) \end{cases} \tag{9}$$

Table 2. Definition of basal performance metrics

Case	Classifier	Truth
True Positive (TP)	Anomaly	Anomaly
True Negative (TN)	Normal	Normal
False Positive (FP)	Anomaly	Normal
False Negative (FN)	Normal	Anomaly

AUC, area under the ROC curve, can provide an overall assessment of the classifier. It ranges in values from 0.5 to 1, where higher value usually represents better overall performance.

Alternative solutions

Nowadays, there are plenty of anomaly-detection algorithms in the domain of data mining. To verify the superiority of the proposed method, a comparative experiment was conducted with other popular algorithms, detailed in the section below.

The selected algorithms are KNN,[38] isolation forest (IForest), minimum covariance determinant (MCD), and histogram-based outlier score (HBOS). KNN is a non-parametric algorithm, which usually detect outliers with distance metrics. IForest is an anomaly-detection algorithm, where outliers are defined as the points more likely to be separated. MCD is a robust estimator, which can identify outliers in multivariate data. HBOS is a histogram-based algorithm, detecting anomalies with the assumption of the feature independence.

All solutions were tested with the same procedure to guarantee fairness. First, the feature vectors for experiments are generated by means of VAE with the same variants ($p = 16$, $l = 25$). Second, there are only positive samples involved in the experiments. Finally, the same approach was adopted to segment defect regions as described in the ''Segmentation of defect regions'' section, except image reconstruction, which was only performed in the proposed method.

Table 3 describes the results of the proposed method and alternative solutions. All metrics were calculated on the 256×256 pixel test images with defects, and these values were obtained when F_2 takes the maximum value with a specific threshold *th*. Results suggest that our method achieves the highest precision 0.733 and F_2 score 0.866. Furthermore, the sensitivity value of 0.907 is superior to 0.867, which was achieved with the method proposed in Silvestre-Blanes et al.[35] In terms of the global goodness, it can be seen obviously that the proposed method outperforms alternatives.

Table 3. Performance metrics of all solutions

Method	Precision	Sensitivity	FPR	F_1	F_2
Proposed	0.733	0.907	0.047	0.810	0.866
GMM	0.518	0.821	0.107	0.635	0.705
KNN	0.404	0.811	0.168	0.539	0.675
IForest	0.376	0.769	0.180	0.505	0.636
MCD	0.280	0.792	0.287	0.413	0.580
HBOS	0.259	0.566	0.100	0.355	0.457

Figure 6 shows the ROC curve for each solution with the corresponding AUC values attached to it. AUC values of all solutions range from 0.829 to 0.982. ROC curves clearly indicate that the suggested solution is more effective for fabric defect detection, yielding the highest AUC value of 0.982. The HBOS method achieves the worst performance, perhaps because of the high-dimensional feature space. In particular, the GMM solution achieves a passable AUC value of 0.929. Thus, we can also infer that the feature vectors extracted from the VAE are really expressive and discriminative, and the detection performance is indeed increased by means of image reconstruction.

Results and discussion

Figure 6 shows the average AUC of the proposed method, which was tested on the 256×256 pixel images. These values were obtained with different patch size p and latent space dimension l as follows:

$$p \in \{8, 16, 32\}, l \in \{10, 15, 20, 25, 30\} \quad (10)$$

Moreover, the optimal number of GMM components was determined by specific BIC.

There are two conclusions that can be drawn from Figure 7. First of all, the proposed method tends to produce higher AUC values with an increase in the dimension of latent space. This is mainly because the number of hidden neurons in VAE has an impact on the ability of feature representation. Although more hidden nodes signify better image features in general, excessive nodes may also result in over-fitting and curse of dimensionality. Second, there is no simple linear relationship between AUC values and patch size. On the one hand, it is hard for a small patch to contain distinctive structural information. On the other hand, the oversize image patch has difficulty in detecting tiny defects and tends to generate larger defect regions. The above-mentioned reasons explain the low AUC values obtained when the patch size was set to 8 or 32. The results also show that the highest AUC value was obtained when the patch size and dimension of latent space were set to 16 and 25, respectively. The best AUC value is approximately 98%.

Figure 8 shows the time cost of the proposed method, which was obtained with the above settings except the test objects. To prove the practicability, the experiments were conducted on a real cloth of 4096×256 pixels. The box plot clearly indicates that the average time cost (943, 561, and 384 ms) decreases with increase in patch size (8, 16, and 32 pixels). With regard to the influence of parameter, the time difference caused by l is less than 200 ms. By contrast, the variation of execution time exceeds 500 ms when merely varying p. In summary, we concluded that patch size has a greater effect on execution time than dimension of latent space. In particular, the time cost is about 0.592 s when considering the best AUC value, which is competent for real-time detection.

Figure 9 shows an example of performing fabric defect detection. Three types of defect forms (broken yarn, contamination, and broken pick) are involved. To achieve better segmentation of defect regions, patch size and latent space dimension were set to 16 and 25,

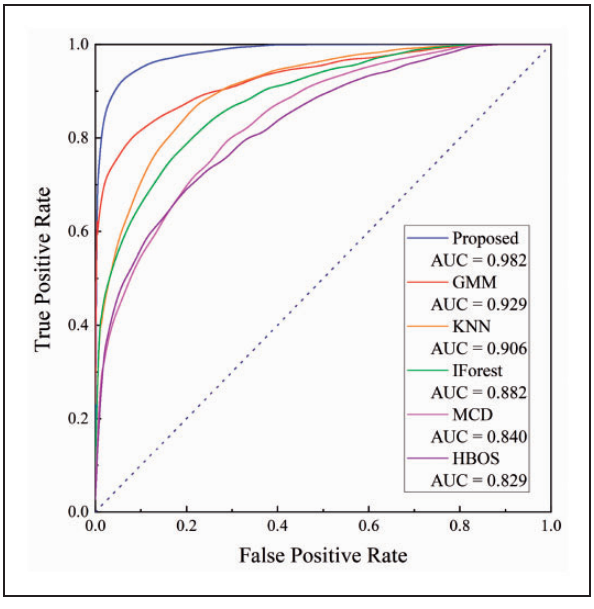

Figure 6. ROC curves for all solutions with a patch size of 16 pixels.

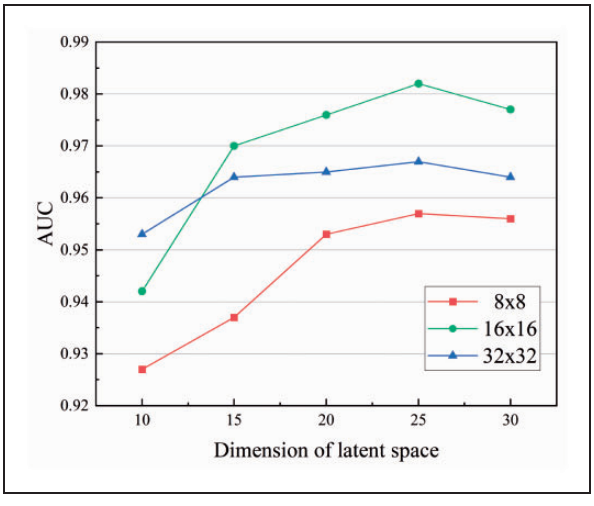

Figure 7. AUC line chart for the proposed method. Values are obtained by varying the dimension of latent space and the patch size.

respectively, according to Figure 7. In the figure below, (a) represents the original samples with defects; (b) and (c) and (d) correspond to the sections ''Reconstruction and feature extraction,'' ''Normal patches model,'' and ''Segmentation of defetct regions,'' respectively; (e) represents the final detection results, where defect regions are green colored. Though the single detection method has many flaws, the proposed hybrid method can provide excellent performance in defect detection. Succinctly, the method can fulfill the requirements of qualitative and quantitative evaluation in automated fabric defect detection.

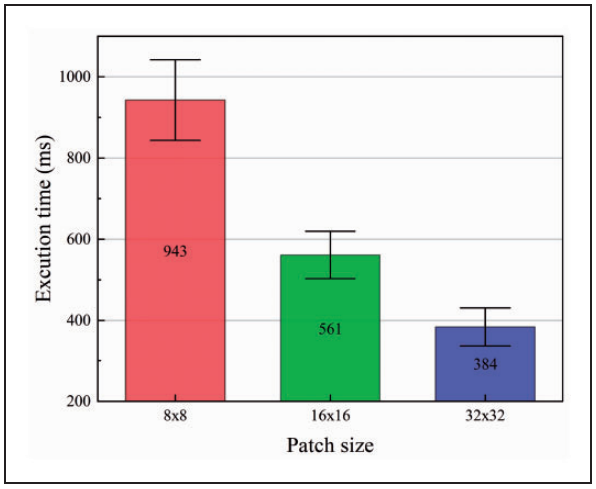

Figure 8. Box-plots reporting the distribution of the execution time with different patch sizes. The experiment was conducted on a real cloth of size 4096×256.

Conclusion

In this paper, we propose a semi-supervised method for fabric defect detection based on VAE and GMM. The VAE model is trained for feature extraction and image reconstruction, and GMM is utilized to perform density estimation. Our method requires only positive samples (i.e. images of fabrics without anomalies) during the training and validation phases. As VAE only learns to reconstruct defect-free fabric images, potential defect regions can be separated from the test image by comparing the original with the reconstructed image. To reduce the influence of noise, SSIM algorithm was employed during comparison. Furthermore, the feature vectors extracted from encoder in VAE were fitted a GMM, which was utilized for density estimation. Hence, the anomaly probability of each image patch can be calculated. In this step, we proposed

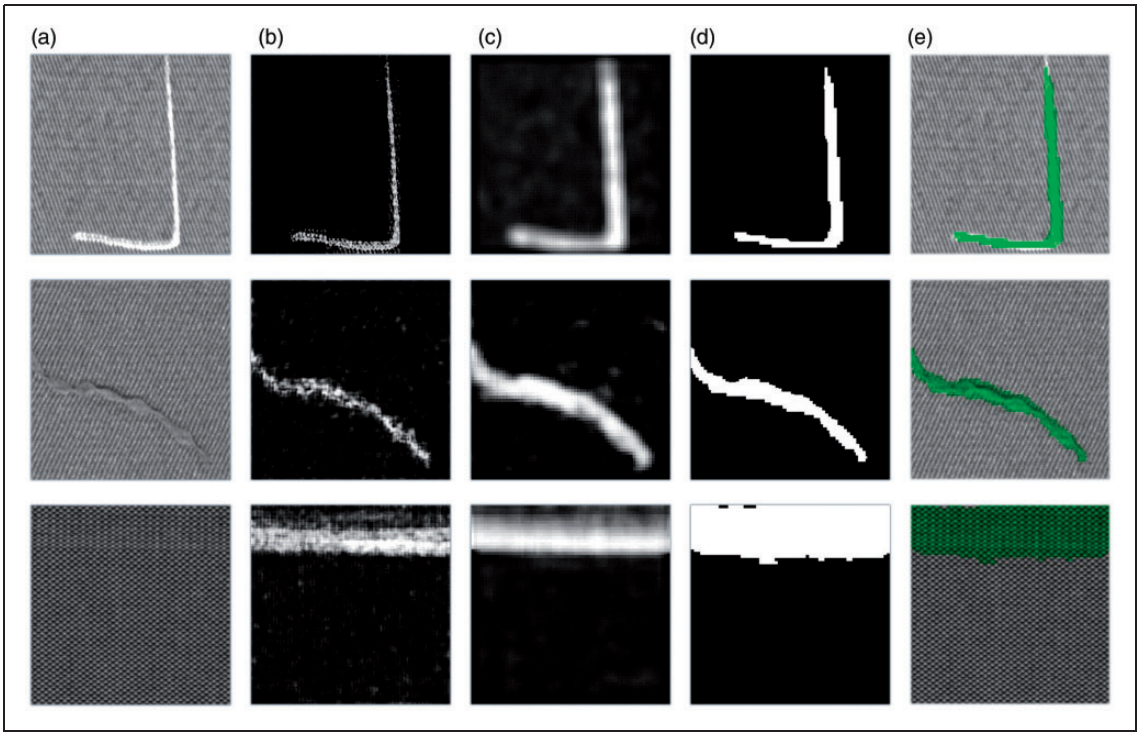

Figure 9. The detection procedure of proposed method: (a) initial input images with defects I; (b) the difference map f_d; (c) the score map f_s; (d) the final segmentation map S obtained by thresholding the probability map f_p, which is a synthesis of f_d and f_s; (e) the detection results of the proposed method, where green pixels represent defect regions.

weighted-HO operator to avoid additional computation caused by excessive number of patches. The two approaches mentioned above generated a difference map and anomaly score map, respectively. Subsequently, the two maps were combined into an anomaly probability map, which was later converted into the final segmentation map by performing a thresholding operation.

The method has been tested on AITEX and DAGM 2007 fabric dataset. We mainly explored the effect of different variants on the model performance. The results suggest that the best performance was obtained when setting a patch size of 16 and latent space dimension of 25. Under these conditions, we obtained an AUC of 0.982, and execution time of 0.592 s, which were tested on real cloth images. The results prove that the method is completely capable of defect detection for quality control in the textile industry. Future investigations could include the measures for illumination change in order to apply the algorithm in real life.

Declaration of conflicting interests

The authors declared no potential conflicts of interest with respect to the research, authorship, and/or publication of this article.

Funding

The authors disclosed receipt of the following financial support for the research, authorship, and/or publication of this article: This work was supported by the National Key R&D Program of China (2017YFB1304000).

ORCID iD

Qihong Zhou https://orcid.org/0000-0001-7140-7762

References

1. Kelkar AD, Tate JS and Bolick R. Structural integrity of aerospace textile composites under fatigue loading. *Mater Sci Eng B* 2006; 132: 79–84.
2. Eyvaz M, Arslan S, Gürbulak E, et al. Textile materials in liquid filtration practices. Current status and perspectives in water and wastewater treatment. *Textil Adv Appl Tech* 2017; 11: 293.
3. Paul R. *High Performance Technical Textiles*. John Wiley & Sons, 2019.
4. Stefanov I, Bassegoda A and Tzanov T. Enzyme biotechnology for medical textiles. In: *Advances in Textile Biotechnology*. Elsevier: 2019, pp.133–158.
5. Yildiz K, Buldu A, Demetgul M, et al. A novel thermal-based fabric defect detection technique. *J Textil Inst* 2015; 106: 275–283.
6. Yıldız K, DemirÖ and Ülkü EE. Fault detection of fabrics using image processing methods. *Pamukkale Univ Muh Bilim Derg* 2017; 23: 841–844.
7. Yildiz K and Buldu A. Wavelet transform and principal component analysis in fabric defect detection and classification. *Pamukkale Univ J Eng Sci* 2017; 23: 622–627.
8. Kumar A. Computer-vision-based fabric defect detection: A survey. *IEEE Trans Ind Electron* 2008; 55: 348–363.
9. Ouyang W, Xu B, Hou J, et al. Fabric defect detection using activation layer embedded convolutional neural network. *IEEE Access* 2019; 7: 70130–70140.
10. Liu Z, Liu S, Li C, et al. Fabric defects detection based on SSD. In: *Proceedings of the 2nd International Conference on Graphics and Signal Processing* 2018, pp.74–78.
11. Jing J, Wang Z, Rätsch M, et al. Mobile-Unet: An efficient convolutional neural network for fabric defect detection. *Textil Res J* 2020: 0040517520928604.
12. Tolba AS. Manifolds for training set selection through outlier detection. In: *The 10th IEEE International Symposium on Signal Processing and Information Technology*. IEEE: 2010, pp.467–472.
13. Napoletano P. Visual descriptors for content-based retrieval of remote-sensing images. *Int J Rem Sens* 2018; 39: 1343–1376.
14. Cusano C, Napoletano P and Schettini R. Combining multiple features for color texture classification. *J Electron Imag* 2016; 25: 061410.
15. Napoletano P, Piccoli F and Schettini R. Anomaly detection in nanofibrous materials by CNN-based self-similarity. *Sensors* 2018; 18: 209.
16. Goodfellow I, Pouget-Abadie J, Mirza M, et al. Generative adversarial nets. In: *Advances in neural information processing systems*. MIT Press: 2014, pp.2672–2680.
17. Haselmann M, Gruber DP and Tabatabai P. Anomaly detection using deep learning based image completion. In: *2018 17th IEEE International Conference on Machine Learning and Applications (ICMLA)*. IEEE: 2018, pp.1237–1242.
18. Zhao Z, Li B, Dong R, et al. A surface defect detection method based on positive samples. In: *Pacific Rim International Conference on Artificial Intelligence*. Springer: 2018, pp.473–481.
19. Schlegl T, Seeböck P, Waldstein SM, et al. Unsupervised anomaly detection with generative adversarial networks to guide marker discovery. In: *International conference on information processing in medical imaging*. Springer: 2017, pp.146–157.
20. Zenati H, Foo CS, Lecouat B, et al. Efficient GAN-based anomaly detection. *arXiv preprint arXiv:180206222* 2018.
21. Akcay S, Atapour-Abarghouei A and Breckon TP. Ganomaly: Semi-supervised anomaly detection via adversarial training. In: *Asian Conference on Computer Vision*. Springer: 2018, pp.622–637.
22. Kingma DP and Welling M. Auto-encoding variational bayes. *arXiv preprint arXiv:13126114* 2013.
23. Reynolds DA. Gaussian Mixture Models. In: *Encyclopedia of biometrics*. Springer: 2009; p.741.
24. Van Looveren A, Vacanti G, Klaise J, et al. Variational auto-encoding gaussian mixture model, https://docs.seldon.io/projects/alibi-detect/en/stable/methods/vaegmm.html (accessed 22 Jul 2020).

25. Hu G, Huang J, Wang Q, et al. Unsupervised fabric defect detection based on a deep convolutional generative adversarial network. *Textil Res J* 2019: 0040517519862880.
26. Wang Z, Bovik AC, Sheikh HR, et al. Image quality assessment: From error visibility to structural similarity. *IEEE Trans Image Process* 2004; 13: 600–612.
27. Tolba AS and Raafat HM. Multiscale image quality measures for defect detection in thin films. *Int J Adv Manuf Technol* 2015; 79: 113–122.
28. Scrucca L, Fop M, Murphy TB, et al. mclust 5: Clustering, classification and density estimation using Gaussian finite mixture models. *R Journal* 2016; 8: 289.
29. Yildiz K. Dimensionality reduction-based feature extraction and classification on fleece fabric images. *Signal Image Video Process* 2017; 11: 317–323.
30. Rumelhart DE, Hinton GE and Williams RJ. Learning representations by back-propagating errors. *Nature* 1986; 323: 533–536.
31. Akaike H. Factor analysis and AIC. In: *Selected papers of Hirotugu Akaike*. Springer: 1987, pp.371–386.
32. Kass RE and Raftery AE. Bayes factors. *J Am Stat Assoc* 1995; 90: 773–795.
33. Papandreou G, Zhu T, Kanazawa N, et al. Towards accurate multi-person pose estimation in the wild. In: *Proceedings of the IEEE Conference on Computer Vision and Pattern Recognition*. IEEE: 2017, pp.4903–4911.
34. Abadi M, Agarwal A, Barham P, et al. Tensorflow: Large-scale machine learning on heterogeneous distributed systems. *arXiv preprint arXiv:160304467* 2016.
35. Silvestre-Blanes J, Albero-Albero T, Miralles I, et al. A public fabric database for defect detection methods and results. *Autex Res J* 2019; 19: 363–374.
36. Wieler M and Hahn T. HCI: Weakly supervised learning for industrial optical inspection, https://hci.iwr.uni-heidelberg.de/node/3616 (accessed 1 May 2020).
37. Jeni LA, Cohn JF and De La Torre F. Facing imbalanced data–recommendations for the use of performance metrics. In: *2013 Humaine association conference on affective computing and intelligent interaction*. IEEE: 2013, pp.245–251.
38. Yıldız K, Buldu A and Demetgul M. A thermal-based defect classification method in textile fabrics with K-nearest neighbor algorithm. *J Ind Textil* 2016; 45: 780–795.